Lab on a Chip

Accepted Manuscript

This is an *Accepted Manuscript*, which has been through the Royal Society of Chemistry peer review process and has been accepted for publication.

Accepted Manuscripts are published online shortly after acceptance, before technical editing, formatting and proof reading. Using this free service, authors can make their results available to the community, in citable form, before we publish the edited article. We will replace this *Accepted Manuscript* with the edited and formatted *Advance Article* as soon as it is available.

You can find more information about *Accepted Manuscripts* in the **Information for Authors**.

ROYAL SOCIETY OF CHEMISTRY

www.rsc.org/loc

A smartphone platform for the quantification of vitamin D levels

Seoho Lee[1], Vlad Oncescu[1], Matt Mancuso[2], Saurabh Mehta[3], David Erickson[1*]

Abstract

1   Vitamin D deficiency has been linked to a number of diseases and adverse outcomes including:

2   osteoporosis, infections, diabetes, cardiovascular diseases, and even cancer. At present the vast majority

3   of vitamin D testing is performed in large-scale laboratories at the request of a physician as part of an

4   annual panel of blood tests. Here we present a system for rapid quantification of vitamin D levels on a

5   smartphone. The system consists of a smartphone accessory, an app, and a test strip that allows the

6   colorimetric detection of 25-hydroxyvitamin D using a novel gold nanoparticle-based immunoassay. We

7   show that the system can be used to accurately measure physiological levels of 25-hydroxyvitamin D with

8   accuracy better than 15nM and a precision of 10nM. We compare our system with well-established

9   ELISA test kits for serum samples of unknown concentration and demonstrate equivalency of the results.

10   We envision this as the first step towards the development of the NutriPhone, a comprehensive system for

11   the analysis of multiple vitamins and micronutrients on a smartphone.

[1] Sibley School of Mechanical and Aerospace Engineering, Cornell University, Ithaca, NY 14853, USA

[2] Department of Biomedical Engineering, Cornell University, Ithaca, NY 14853, USA

[3] Division of Nutritional Sciences, Cornell University, Ithaca, NY 14853, USA

*de54@cornell.edu

Introduction

1   Vitamin D deficiency is prevalent worldwide[1] and has been linked to diabetes[2], cardiovascular diseases[3, 4],

2   infections[5, 6], and cancer[7, 8] in addition to bone diseases such as osteoporosis[9] and rickets[10]. Deficiency is

3   commonly defined in humans by measuring serum concentrations of 25-hydroxyvitamin D, or 25(OH)D,

4   the circulating form of vitamin D. The currently recommended cutoffs for vitamin D deficiency and

5   insufficiency are defined by 25(OH)D levels below 50nM and 80nM respectively. Low levels of vitamin

6   D can usually be improved by consuming supplements and increasing skin exposure to sunlight.[11]

7   However, many people are unaware of their vitamin D status due to the lack of simple methods for

8   diagnosing and tracking 25(OH)D concentrations in the blood. The ability to monitor vitamin D levels

9   may help those at risk to detect low levels at an earlier stage and enable corrective interventions before

10   the occurrence of potentially irreversible damage. Reliance on supplements alone without knowledge of

11   true vitamin D status may fall short in addressing severe vitamin D deficiencies (<20nM) or in some cases

12   lead to possible vitamin D intoxication.[11, 12] At present, most 25(OH)D tests are conducted using high-

13   performance liquid chromatography (HPLC), liquid chromatography-tandem mass spectrometry (LC-

14   MS) techniques, or certain immunoassays such as radioimmunoassay (RIA) and enzyme-linked

15   immunosorbent assay (ELISA).[13-15] These methods are time consuming, costly and difficult to perform in

16   most settings outside sophisticated laboratories. Recently, a lateral flow assay for vitamin D (Test4D;

17   Nanospeed Diagnostics) has been introduced[16], demonstrating the commercial need for such rapid, point-

18   of-care vitamin D analysis. Smartphone based diagnostics offer additional advantages over lateral flow

19   assays including the abilities to quantify results, track changes with time, and provide user-free error

20   tracking.

21   We present here the vitaAID – _vita_min AuNP-based Immunoassay Device – a system for rapid

22   quantification of vitamin D levels on a smartphone. This is achieved through the development of: a

23   smartphone accessory, app, and novel gold nanoparticle (AuNP) based colorimetric competitive direct-

24   antigen immunoassay. This assay enables us to quantify 25(OH)D molecules whose small size

25   (~400g/mol) restricts their binding to more than one antibody at a time.[17, 18]. Gold nanoparticle based

26   colorimetric assays[19, 20] coupled with smartphone technology have previously been used for the

27   quantification of mercury contamination in water samples as demonstrated by Wei _et al._[21] In addition,

28   smartphone platforms were used for the detection of biomarkers in complex bodily fluids[22-25], thereby

29   demonstrating the ability to do rapid, personalized diagnostics.

30   In this paper we describe the vitaAID and show how 25(OH)D levels can be quantified by evaluating

31   brightness differences between the detection area and a reference area on the vitaAID test strip. We then

32   demonstrate that the vitaAID system can be used to quantify vitamin D levels by evaluating serum

33   samples with unknown 25(OH)D concentrations and comparing the results to those obtained using a

34   commercial ELISA method.

Results

1   **vitaAID system and test strip surface chemistry.** The vitaAID system consists of a smartphone

2   accessory and custom test strip as shown in Fig. 1a. The accessory has been designed to minimize the

3   effect of variability in external lighting conditions with a 5mm amber LED (λ=592nm) embedded in a

4   polydimethylsiloxane (PDMS) diffuser used to illuminate the back of the test strip. The test strip is

5   composed of a detection area and reference area. The reference area allows the algorithm to further adjust

6   to differences in smartphone cameras. The detection area that enables the colorimetric reaction to occur

7   consists of a surface-immobilized layer of 25(OH)D. There is currently no standard method for obtaining

8   a chemically stable coating layer of 25(OH)D due to the small size and absence of linkable functional

9   groups on the 25(OH)D. We addressed this by developing a novel 25(OH)D coating process onto a fused

10   Si-based substrate that serves as the detection area on the test strip. As shown in Fig. 1b, we coated the 3-

11   aminopropyltriethoxysilane (APTES) and polystyrene-*co*-maleic anhydride (PSMA) layers sequentially

12   on a fused Si substrate and covalently linked aminopropylated 25(OH)D to achieve a stable 25(OH)D

13   coating. In order to validate this method, the surface treatments were characterized by Fourier-transform

14   infrared spectroscopy (FT-IR) as shown in Fig. 1b. The initial introduction of APTES layer on the Si

15   substrate is evident from the transmittance peak at 1654cm^{-1} that is associated with primary amine groups

16   (-NH$_2$).[26] The PSMA coating is confirmed by the appearance of peaks at 1850 and 1780cm^{-1} which have

17   been linked with maleic anhydrides in other studies.[26-28] Lastly, the peak at 3300cm^{-1} corresponds to the

18   formation of the secondary amine (R$_2$NH) bond between the PSMA and aminopropylated 25(OH)D and

19   verifies the 25(OH)D immobilization.[29]

1   **Surface-based gold nanoparticle immunoassay.** The colorimetric reaction on the detection area of the

2   test strip is based on a novel surface-based gold nanoparticle-based immunoassay as shown in Fig. 2a.

3   When a sample is applied onto the detection area of the test strip, only the antibody conjugates that are

4   not bound to the 25(OH)D present in the initial sample are captured by the coated 25(OH)D on the

5   surface. The colorimetric signals from the immobilized AuNP-antibody conjugates are then amplified

6   using a silver enhancement scheme as the silver ions undergo reduction on the surface of the AuNP to

7   increase their size and thereby increase the sensitivity of the system. For samples with high vitamin D

8   levels, most of the antibody conjugates are occupied with 25(OH)D from the initial sample, resulting in

9   only a subtle change in the colorimetric signal on the test strip. For samples with low vitamin D levels,

10   the test strip develops an intense color that reflects the high number of antibody conjugates bound on the

11   surface. The steps involved in the preparation of the AuNP-anti-25(OH)D conjugate solution and the

12   detection area are discussed in the Methods section.

13   A critical step during testing is the incubation of the AuNP-anti-25(OH)D sample solution on the test

14   strip's detection area. It is important to characterize the time it takes for the AuNP-anti-25(OH)D to

15   immobilize in order to minimize the total assay time and to improve accuracy. In Fig. 2b ,we show the

16   effect of different incubation times on the brightness difference between the detection and reference areas

17   of the test strip (ΔH) for a sample without 25(OH)D. After 6h the brightness difference is within 10% of

18   that obtained after a typical 12h overnight incubation. This indicates that a 6h incubation time is sufficient

19   in order to obtain accurate results during such vitamin D measurements. The incubation time can however

20   be significantly reduced by using the obtained negative exponential relationship to determine the

21   minimum incubation time for ensuring that sufficient conjugate binding events have occurred on the

22   detection area. In a recent study, Kai *et al*.[30] have demonstrated that the incorporation of microfluidic

23   channels could further reduce such incubation times to the order of minutes through improved binding

24   kinetics.

1   **Quantification of colorimetric reaction.** Once the competitive binding of AuNP-anti-25(OH)D was

2   performed on the test strip, the quantification of the 25(OH)D levels in the initial sample can be achieved

3   using the vitaAID smartphone platform. First, the colorimetric change is captured using the smartphone's

4   camera after inserting the test strip in the vitaAID accessory. In Fig. 3a we show the colorimetric change

5   in the transparent fused silica detection region at different known concentrations of 25(OH)D and the

6   colorimetric change on the white reference region due to changes in exposure time of the camera. The

7   iPhone automatically adjusts its camera exposure times in response to the amount of light passing through

8   the detection region. Therefore, by comparing the differences in brightness between the detection area

9   (B_{det}) and reference area (B_{ref}) we can estimate the concentration of 25(OH)D independent of the exposure

10   setting of the iPhone camera. In Fig. 3b we show that $\Delta H = B_{det} - B_{ref}$ can be correlated to the 25(OH)D

11   concentration in the initial sample. A second order polynomial was then fitted onto this calibration curve

12   in order to obtain a function such that $[25(OH)D] = f(\Delta H)$.

13   Fig. 3c shows the algorithm that allows the quantification of 25(OH)D across the entire range of

14   physiological values. First, the detection area is scanned for silver enhanced regions where AuNP-anti-

15   25(OH)D is bound. This is important because at higher 25(OH)D concentrations in the initial sample, the

16   detection area rarely exhibits a uniform colorimetric change. A 100px by 100px area around the high

17   intensity silver enhanced region is taken and the brightness is averaged across all the pixels in that area.

18   The brightness is a coordinate in the Hue Saturation Brightness (HSB) color model and is computed from

19   the Red Green Blue (RGB) average values as described elsewhere.[31] The same steps are then performed

20   on the reference region and an average brightness is calculated. Once the brightness difference between

21   the detection area and the reference area is computed, the algorithm uses a second order polynomial

22   [25(OH)D] = f(ΔH) derived from Fig. 3b to calculate the 25(OH)D concentration in the initial sample.

1

1   **Accuracy and precision compared to ELISA.** The accuracy of the vitaAID system was characterized by

2   quantifying 25(OH)D levels in solutions of known concentrations and comparing them to results obtained

3   using a commercial ELISA kit. In Fig. 4a we show variations in predicted 25(OH)D levels for 3 standard

4   solutions of 15nM, 40nM and 110nM. At each concentration, 3 test strips were used and the maximum

5   error across all the samples and concentrations was measured as 14.1nM at a concentration of 40nM. The

6   maximum average inter-sample difference was 9.8nM also at 40nM. These errors are of the same order as

7   those of ELISA methods for the quantification of 25(OH)D levels.

8   In Fig. 4b, 3 serum samples of unknown 25(OH)D concentration are evaluated using both the vitaAID

9   system and an ELISA method. As indicated previously, 25(OH)D levels below 50nM indicate vitamin D

10   deficiency while level below 20nM indicate a severe deficiency. Both methods are in agreement that 2 of

11   the samples are 25(OH)D deficient, while the other is borderline deficient. Moreover, 2 of the ELISA

12   measurements fall within the range of values measured using the vitaAID system and one is within 2nM

13   of that range.

Discussion

1   In this paper we presented the vitaAID system which allows for the fast and accurate quantification of

2   25(OH)D levels. This system uses a novel gold nanoparticle-based immunoassay in order to produce a

3   surface colorimetric reaction that can be quantified directly on a smartphone. We have demonstrated that

4   we can measure physiological levels of 25(OH)D in solution with accuracy better than 15nM and a

5   precision of 10nM. Moreover we show that the results obtained using the vitaAID system are comparable

6   with that of commercial ELISA kits. By analyzing 3 serum samples with unknown 25(OH)D

7   concentration we were able to determine accurately the extent of vitamin D deficiency in each case. These

8   results represent a promising step in the development of an accurate system for determining vitamin D

9   levels which has many potential applications as a point-of-care tool both in the developed and the

10   developing world.

11   In the future, this method for vitamin D quantification can be further improved in terms of precision and

12   accuracy. Here, we used a specific form of 25(OH)D for coating and detection, namely 25(OH)D$_3$ and

13   anti-25(OH)D$_3$. The monoclonal anti-25(OH)D$_3$ has 68% cross reactivity with 25(OH)D$_2$ and 100% with

14   25(OH)D$_3$. The use of 25(OH)D$_3$ for the detection zone coating allows for the capturing of all the

15   unbound AuNP-anti-25(OH)D$_3$ conjugates after the initial interaction with the sample. Nonetheless, this

16   difference in the antibody affinity inevitably causes our method to underestimate the total 25(OH)D level

17   which is the sum of the 25(OH)D$_2$ and 25(OH)D$_3$ levels. This represents the shortcoming of most

18   immunoassays for vitamin D (e.g. ELISA kit; Alpco, radioimmunoassay; DiaSorin) as demonstrated

19   through clinical comparison studies with other detection standards such as HPLC and LC-MS.[13, 14, 32]

Methods

1   **Sample preparation.** For a vitamin D deficiency test, once the sample has been acquired, several steps

2   are performed in solution prior to its application onto the vitaAID test strip. First, the filtered serum

3   sample is mixed 1:10 (v/v) with 0.78g/ml acetonitrile (Thermo Fisher Sceintific Inc.) in order to liberate

4   the 25(OH)D molecules that are in proportion of 95-99% bound to vitamin D binding proteins (DBP).[33, 34]

5   The sample is then mixed with AuNP-anti-25(OH)D conjugate solution for 30min. This ensures that all

6   the 25(OH)D initially present in the blood sample is bound to AuNP-anti-25(OH)D before being applied

7   onto the test strip.

1   **AuNP-anti-25(OH)D$_3$ conjugate preparation.** The spherical AuNP (Nanopartz Inc., 30nm) came pre-

2   treated with N-hydroxysuccinimide ester terminal (NHS) groups which specifically reacted with the

3   primary amines of monoclonal anti-25(OH)D$_3$ IgG (Raybiotech Inc.) to form the AuNP-antibody

4   conjugates. The antibody was first purified using the Pierce Antibody Clean-up Kit (Thermo Fisher

5   Scientific Inc.) because 2% bovine serum albumin (BSA) stabilizers in anti-25(OH)D$_3$ are known to

6   interfere with the amine-reactive conjugation.[35] The antibody solution was placed into the Melon Gel-

7   based purification support which binds non-antibody proteins while allowing the IgG antibody to flow

8   through in a purified form during the one-minute centrifugation at 6000g. The successful removal of BSA

9   was checked by performing sodium dodecyl sulfate polyacrylamide gel electrophoresis (SDS-PAGE). For

10   conjugation, the AuNP were mixed with the purified anti-25(OH)D$_3$ at 0.1mg/ml in 0.01M amine-free

11   phosphate buffer saline (PBS) buffer at pH 7.4. The mixture was sonicated for 30s to re-suspend AuNP

12   into solution, followed by vortexing for 30min at room temperature.[36] The centrifugation was performed

13   at 15000g for 10min to remove the excess antibody in supernatant form and the final conjugates were

14   reconstituted in 0.01M PBS with 0.1% Tween-20 at pH 7.4. The successful conjugation was confirmed

15   through surface plasmon resonance changes using ultraviolet-visible spectroscopy. The conjugates were

16   diluted to 10µg/ml and stored at 4°C until use.

1   **Detection area preparation.** The covalent immobilization of 25(OH)D was achieved by obtaining

2   25(OH)D$_3$, 3'-Aminopropyl Ether (Toronto Research Chemicals Inc.) and using its primary amines as

3   linkers to the test strip surface. Immobilization of the peptides to surface using maleic anhydride

4   chemistry has been demonstrated previously by others.[37, 38] Here, the aminopropylated 25(OH)D$_3$ was

5   immobilized on a flat Si substrate other than on a typical well-plate which represents a compatibility

6   improvement for use in our smartphone-based detection. Briefly, 4" fused Si wafers were cleaned in

7   piranha solution, immersed in 20mM APTES (Sigma-Aldrich Co. LLC) in isopropanol for 2h and

8   annealed at 120°C for 1h. The APTES coating acted as an activation layer for the binding of 1% PSMA

9   (Sigma-Aldrich Co. LLC) dissolved in tetrahydrofuron, which was spin-coated at 3500rpm for 30s

10   followed by curing at 120°C for 2h. The treated Si wafer was cooled and immersed in acetone for 10min

11   and subsequently diced into 4 by 7mm strips. Finally, the 25(OH)D immobilization was achieved by

12   incubating the PSMA-treated strips with 20µg/ml aminopropylated 25(OH)D$_3$ in the coating buffer (0.1M

13   carbonate/bicarbonate buffer at pH 9.4) for 1h at 37°C. The unreacted PSMA sites were treated by

14   incubating the blocking buffer (0.01M PBS with 1mg/ml Casein and 0.05% Kathon preservative at pH

15   7.4) for 30min at room temperature, and cleaned with washing buffer (0.01M PBS with 0.05% Tween-20

16   at pH 7.4). The incubation procedures were performed in custom incubation chambers that housed the test

17   strips and prevented pre-mature drying of the treatment solutions. The modified Si surfaces after each

18   surface treatment were characterized by FT-IR using a Vertex 80-v spectrometer (Bruker Optics)

19   equipped with a 60° germaniam attenuated total reflection (VeeMax Ge ATR) crystal. For each spectrum,

20   256 scans at a spectral resolution of 4cm^{-1} were performed using a liquid nitrogen detector. After the 6h

21   incubation of AuNP-antibody conjugates with the sample on the detection area, the strip was rinsed three

22   times with the washing buffer to remove unbound conjugates and incubated with silver enhancement

23   solution from the Silver Enhancer Kit (Sigma-Aldrich Co. LLC). After 20min, the detection area was

24   rinsed with the washing buffer and air dried at room temperature.

1   **ELISA kit procedures.** The standard and serum samples were analyzed with 25-OH Vitamin D ELISA

2   kit (ALPCO Diagnostics) according to the provided protocol. Briefly, the samples were incubated with

3   the releasing agent to separate 25(OH)D molecules from DBP at 37°C for 1h. The samples and anti-

4   25(OH)D were then added onto the 25(OH)D coated microtiter plates. During an overnight (18-22h)

5   incubation, the 25(OH)D molecules in the sample and those immobilized on the plates competitively

6   bound to the available anti-25(OH)D. The plates were washed to remove any unbound anti-25(OH)D and

7   peroxidase-conjugated antibody were added to form 25(OH)D─anti-25(OH)D─peroxidase antibody

8   complex on the plate surface. After 1h incubation, the plates were washed and tetramethylbenzidine

9   (TMB) substrates were added which resulted in a reaction causing the solution color to change. After

10   20min, the reaction was stopped with an acidic solution and the absorption of the solution was measured

11   using Spectramax 384 at 450nm.
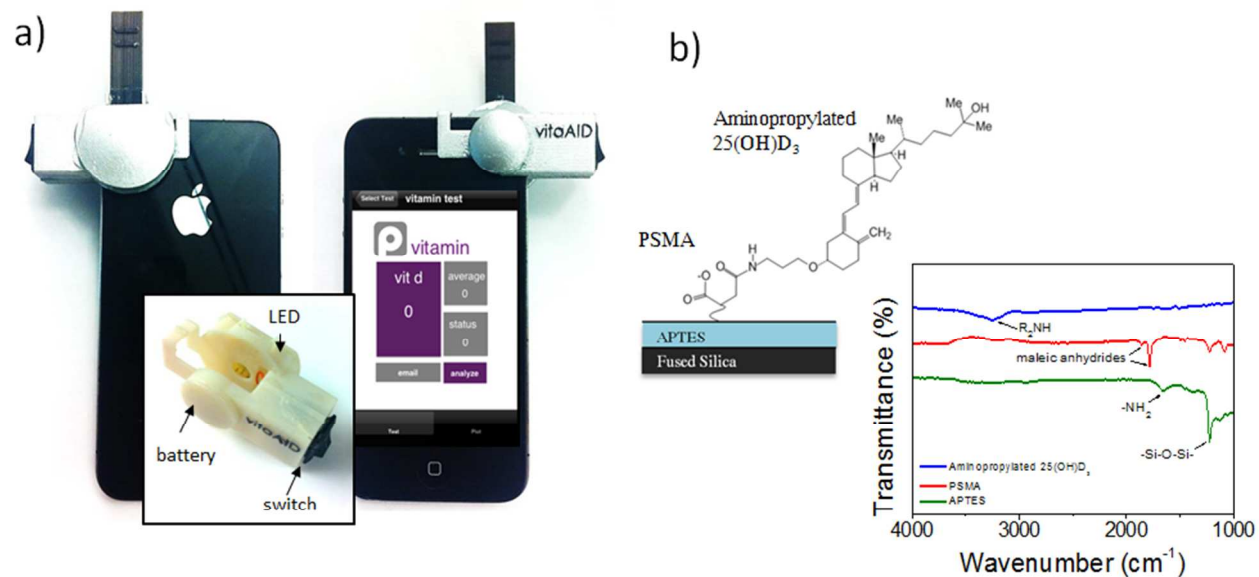
Acknowledgments

Figure 1 a) vitaAID accessory on a iPhone with the inset showing the components of the accessory b) FT-IR spectra showing the chemical composition of the APTES, maleic anhydride and aminopropylated 25(OH)D₃ layers that constitute the detection area
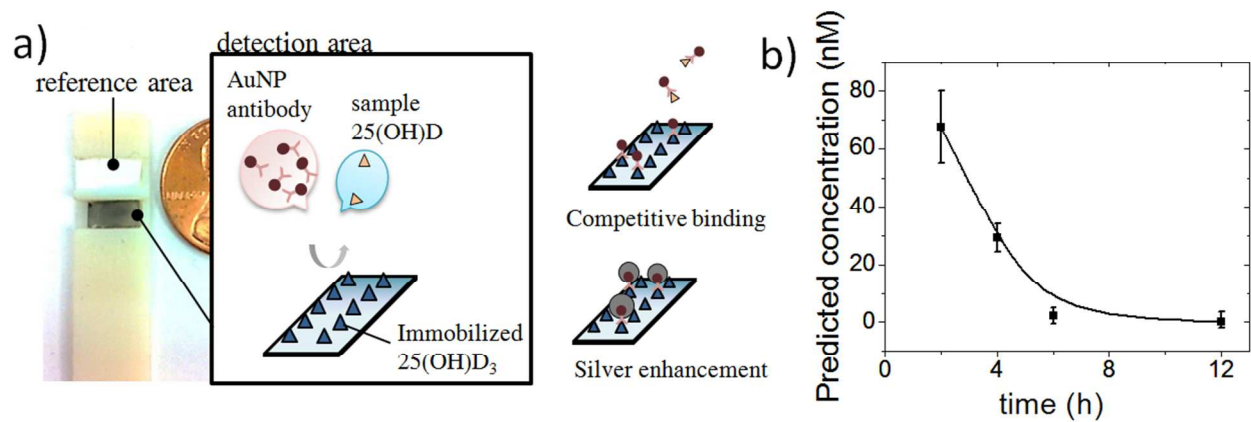
Figure 2 a) Test strip and schematic of the gold nanoparticle-based immunoassay reaction on the detection area b) variation in predicted concentration at different AuNP-anti-25(OH)D_3 incubation times on the detection area for 0nM sample 25(OH)D
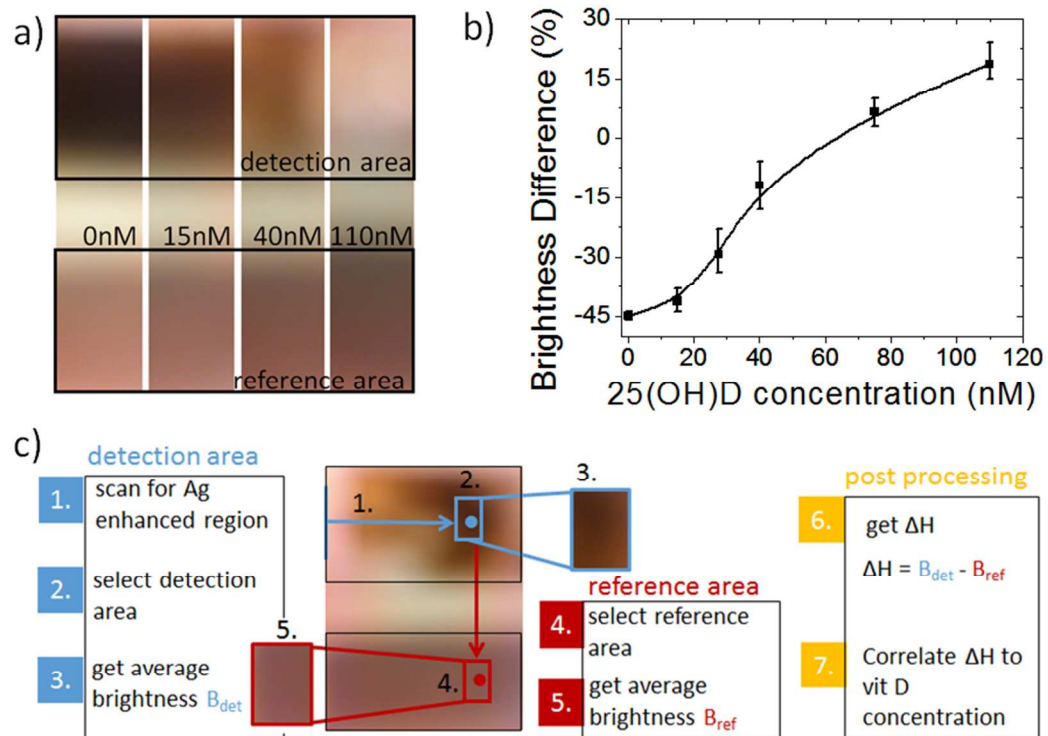
Figure 3 a) colorimetric variation on the test strip at different known 25(OH)D concentrations b) calibration curve showing brightness difference between the detection area and reference area ΔH at different known 25(OH)D concentrations c) algorithm used in quantifying 25(OH)D levels on test strip
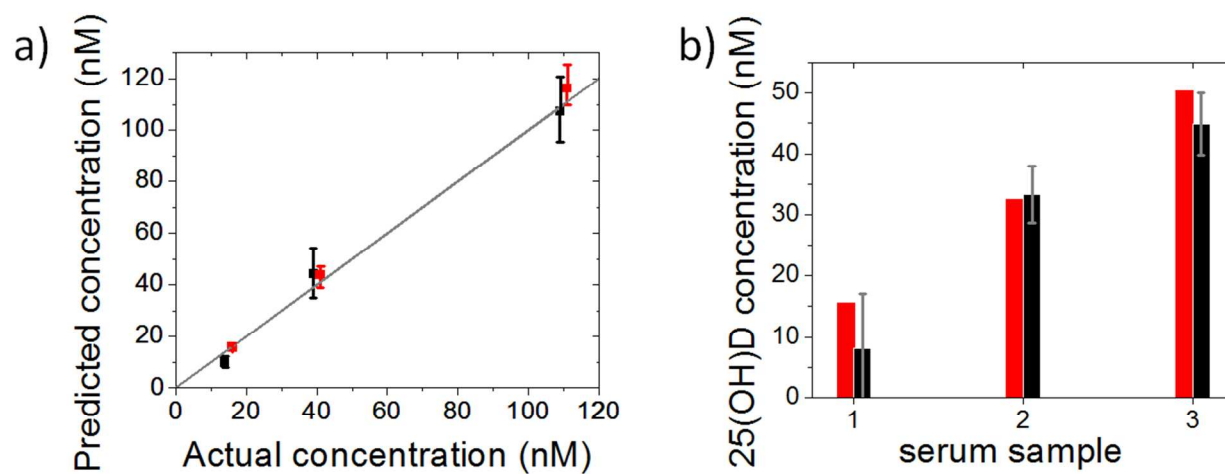
Figure 4 a) predicted concentration vs. actual concentration (grey line) for calibration solutions at 15nM, 40nM and 110nM using vitaAID system (black) and ELISA kit (red) b) predicted concentrations of 25(OH)D in serum samples and comparison to the average ELISA result

Reference

1.   M. F. Holick, *N Engl J Med*, 2007, 357, 266-281.
2.   M. F. Holick, *The American Journal of Clinical Nutrition*, 2004, 79, 362-371.
3.   T. J. Wang, M. J. Pencina, S. L. Booth, P. F. Jacques, E. Ingelsson, K. Lanier, E. J. Benjamin, R. B. D'Agostino, M. Wolf and R. S. Vasan, *Circulation*, 2008, 117, 503-511.
4.   J. L. Anderson, H. T. May, B. D. Horne, T. L. Bair, N. L. Hall, J. F. Carlquist, D. L. Lappe and J. B. Muhlestein, *The American journal of cardiology*, 2010, 106, 963-968.
5.   S. Mehta, E. Giovannucci, F. M. Mugusi, D. Spiegelman, S. Aboud, E. Hertzmark, G. I. Msamanga, D. Hunter and W. W. Fawzi, *PLoS ONE*, 2010, 5, e8770.
6.   S. Mehta, D. J. Hunter, F. M. Mugusi, D. Spiegelman, K. P. Manji, E. L. Giovannucci, E. Hertzmark, G. I. Msamanga and W. W. Fawzi, *The Journal of infectious diseases*, 2009, 200, 1022-1030.
7.   C. F. Garland, F. C. Garland, E. D. Gorham, M. Lipkin, H. Newmark, S. B. Mohr and M. F. Holick, *American Journal of Public Health*, 2006, 96, 252-261.
8.   J. M. Lappe, D. Travers-Gustafson, K. M. Davies, R. R. Recker and R. P. Heaney, *The American Journal of Clinical Nutrition*, 2007, 85, 1586-1591.
9.   M. XunWu, *Zhongguo Shiyong Neike Zazhi/Chinese Journal of Practical Internal Medicine*, 2009, 29, 965-967.
10.   R. Chesney, *Rev Endocr Metab Disord*, 2001, 2, 145-151.
11.   P. Lips, *J Steroid Biochem Mol Biol*, 2010, 121, 297-300.
12.   A. Mithal, D. A. Wahl, J. P. Bonjour, P. Burckhardt, B. Dawson-Hughes, J. A. Eisman, G. El-Hajj Fuleihan, R. G. Josse, P. Lips and J. Morales-Torres, *Osteoporos Int*, 2009, 20, 1807-1820.
13.   H. J. Roth, H. Schmidt-Gayk, H. Weber and C. Niederau, *Annals of clinical biochemistry*, 2008, 45, 153-159.
14.   A. M. Wallace, S. Gibson, A. de la Hunty, C. Lamberg-Allardt and M. Ashwell, *Steroids*, 2010, 75, 477-488.
15.   B. W. Hollis and R. L. Horst, *The Journal of Steroid Biochemistry and Molecular Biology*, 2007, 103, 473-476.
16.   R. Gupta and S. Gupta, *Lateral flow immunoassay for detecting vitamins*, Report WO/2012/129650, 2012.
17.   E. Fu, K. E. Nelson, S. A. Ramsey, J. O. Foley, K. Helton and P. Yager, *Anal Chem*, 2009, 81, 3407-3413.
18.   P. Pradelles, J. Grassi, C. Creminon, B. Boutten and S. Mamas, *Anal Chem*, 1994, 66, 16-22.
19.   K. Lei and Y. C. Butt, *Microfluid Nanofluid*, 2010, 8, 131-137.
20.   C.-H. Yeh, C.-Y. Hung, T. Chang, H.-P. Lin and Y.-C. Lin, *Microfluid Nanofluid*, 2009, 6, 85-91.
21.   Q. Wei, R. Nagi, K. Sadeghi, S. Feng, E. Yan, S. J. Ki, R. Caire, D. Tseng and A. Ozcan, *ACS nano*, 2014.
22.   A. F. Coskun, R. Nagi, K. Sadeghi, S. Phillips and A. Ozcan, *Lab on a Chip*, 2013, 13, 4231-4238.
23.   A. F. Coskun, J. Wong, D. Khodadadi, R. Nagi, A. Tey and A. Ozcan, *Lab on a Chip*, 2013, 13, 636-640.
24.   V. Oncescu, M. Mancuso and D. Erickson, *Lab on a Chip*, 2014, 14, 759-763.
25.   V. Oncescu, D. O'Dell and D. Erickson, *Lab on a Chip*, 2013, 13, 3232-3238.
26.   J. H. Wang, L. P. Zhu, B. K. Zhu and Y. Y. Xu, *J Colloid Interface Sci*, 2011, 363, 676-681.
27.   G. C. Chitanu, I. Popescu and A. Carpov, *Revue Roumaine de Chimie*, 2006, 51, 923-929.
28.   J.-H. Jeong, Y.-S. Byoun and Y.-S. Lee, *Reactive and Functional Polymers*, 2002, 50, 257-263.
29.   R.-H. Lin and J.-H. Hsu, *Polymer international*, 2001, 50, 1073-1081.

30.   J. Kai, A. Puntambekar, N. Santiago, S. H. Lee, D. W. Sehy, V. Moore, J. Han and C. H. Ahn, *Lab on a Chip*, 2012, 12, 4257-4262.
31.   J. Bigun, in *Vision with Direction: A Systematic Introduction to Image Processing and Computer Vision*, Springer, Germany, 2006, ch. 2, pp. 31-32.
32.   C. S. Højskov, L. Heickendorff and H. J. Møller, *Clinica Chimica Acta*, 2010, 411, 114-116.
33.   A. M. Wootton, *Clinical Biochemist Reviews*, 2005, 26, 33.
34.   G. D Carter, *Current drug targets*, 2011, 12, 19-28.
35.   A. C. Grodzki and E. Berenstein, in *Immunocytochemical Methods and Protocols*, Springer, 2010, pp. 15-26.
36.   J. Ljungblad, Linköping University, Department of Physics, Chemistry and Biology, 2009.
37.   M. Tasso, A. L. Cordeiro, K. Salchert and C. Werner, *Macromolecular bioscience*, 2009, 9, 922-929.
38.   A. L. Cordeiro, T. Pompe, K. Salchert and C. Werner, in *Bioconjugation Protocols*, Springer, 2011, pp. 465-476.